tion cross section. In this interpretation the internal electric fields[19,22] make the glasses more transparent than a crystal with the same concentration of states in the gap. One can roughly visualize the nature of the effect with the following picture. As the percolation theory suggests,[23] above the mobility edge, but close to it, the extended states do not exist in the whole volume V_s of the sample but only in a part V_s' (Fig. 5). If we neglect transitions between states located at different sites, the absorption is reduced by a factor V_s'/V_s.

ACKNOWLEDGMENTS

We are grateful to Miss B. E. Prescott and J. Waszczak for technical assistance, and to Professor J. D. Dow and Dr. A. Menth for many helpful discussions. We thank Professor H. Fritzsche and Dr. P. Nielsen for the preprints of their papers.

[1]M. L. Theye, Mater. Res. Bull. 6, 103 (1971).
[2]J. E. Davey and T. Pankey, J. Appl. Phys. 40, 212 (1969).
[3]T. M. Donovan, W. E. Spicer, J. M. Bennett, and E. J. Ashley, Phys. Rev. B 2, 397 (1970).
[4]J. Tauc, in *The Optical Properties of Solids*, edited by F. Abeles (North-Holland, Amsterdam, 1971).
[5]E. A. Davis and N. F. Mott, Phil. Mag. 22, 903 (1970).
[6]A. Vaško, in *Physics of Selenium and Tellurium*, edited by W. C. Cooper (Pergamon, New York, 1969), p. 241.
[7]J. T. Edmond, Brit. J. Appl. Phys. 17, 979 (1966).
[8]E. L. Zorina, Opt. i Spektroskopiya 27, 320 (1969) [Opt. Spectry. (USSR) 27, 168 (1969)]; P. A. Young, J. Phys. C 4, 93 (1971). These two authors ascribe the weak absorption tails (which they observed at absorption levels very different from each other) to indirect phonon-assisted transitions. However, the observed temperature dependence cannot be explained by the current theory of such transitions.
[9]J. Tauc and A. Menth, Bull. Phys. Soc. 15, 553 (1970).
[10]A. Menth, F. DiSalvo, and J. Tauc (unpublished).
[11]A. R. Tynes, Appl. Opt. 9, 2706 (1970).
[12]N. F. Mott, Phil. Mag. 13, 989 (1966).
[13]M. H. Cohen, H. Fritzsche, and S. R. Ovshinsky, Phys. Rev. Letters 22, 1065 (1969).
[14]J. Tauc, A. Menth, and D. L. Wood, Phys. Rev. Letters 25, 749 (1970).
[15]B. T. Kolomiets, T. F. Mazets, and Sh. M. Efendiev, J. Non-Cryst. Solids 4, 95 (1970).
[16]D. M. Eagles, J. Phys. Chem. Solids 16, 76 (1960).
[17]N. K. Hindley, J. Non-Cryst. Solids 5, 17 (1970).
[18]J. Tauc, Mater. Res. Bull. 5, 721 (1970).
[19]J. D. Dow and D. Redfield, Phys. Rev. Letters 26, 762 (1971).
[20]J. D. Dow and J. J. Hopfield, Proceedings of the Fourth International Conference on Amorphous and Liquid Semiconductors, Ann Arbor, Mich., 1971 (unpublished).
[21]P. Nielsen, Solid State Commun. 9, 1745 (1971).
[22]H. Fritzsche, J. Non-Cryst. Solids 6, 49 (1971).
[23]M. H. Cohen, J. Non-Cryst. Solids 4, 391 (1970).

PHYSICAL REVIEW B VOLUME 5, NUMBER 8 15 APRIL 1972

Phonon Density of States in Germanium at 80 K Measured by Neutron Spectrometry

G. Nelin and G. Nilsson
Aktiebolaget Atomenergi, Studsvik, Sweden
(Received 29 July 1971)

More than 500 frequencies of phonons with reduced wave vectors evenly distributed over an irreducible section of the first Brillouin zone have been measured in germanium at 80 K with a neutron crystal spectrometer. The phonon density of states was calculated from the data with an improved sampling technique. Comparisons between thermodynamic quantities derived from calorimetric data and from the present spectrum reveal an excellent agreement. A critical-point scheme determined by use of a method originating from Phillips is also presented. The scheme properly satisfies the Morse relations and other topological conditions, and most of the van Hove singularities expected are clearly displayed in the spectrum.

I. INTRODUCTION

The phonon density of states $g(\nu)$ of a crystalline solid is defined as follows. The function $g(\nu)d\nu$ signifies the fraction of the total number of phonon states in the frequency interval $(\nu, \nu+d\nu)$ if $\int g(\nu)d\nu$ is normalized to 1. Knowledge of $g(\nu)$ is essential for understanding of the thermodynamic properties, for extraction of the electron-phonon coupling coefficient in a tunnel-junction experiment, for design of reactor moderators, etc. It is difficult to make good direct measurements of the density of states, and few spectra have actually been studied. Usually measurements reveal only the main peaks.

Theoreticians have produced mathematically accurate $g(\nu)$ functions for lattice models in about two decades, and one of the most striking results of these calculations is the existence of kinks in $g(\nu)$ or discontinuities in $dg/d\nu$. Van Hove[1] pointed out that they originate from so-called critical points in the $\nu(\vec{q})$ branches ($\vec{q}$ is the phonon wave vector).

A common technique for obtaining $g(\nu)$ is to measure the phonon dispersion relations for some principal symmetry directions on a single crystal with a three-axis crystal spectrometer, fit a lattice dynamical model to the data, and calculate frequencies for off-symmetry directions.[2] The accuracy of this method hinges on the validity of the model applied. When the frequencies of a large number of uniformly distributed phonons are known, $g(\nu)$ is obtained by sampling the phonons in suitable frequency intervals. As no model available to us afforded a satisfactory fit to the data in the principal symmetry directions of germanium, we have extended an earlier investigation[3] to include off-symmetry phonons as well. (By a satisfactory fit we mean a fit within the experimental error of every frequency.) Then we were able to sample the density of states directly from the measured frequencies. This procedure has previously been applied by Stedman *et al.*[4] to aluminium and lead. It is accurate, but time consuming. In the present work the sampling procedure is improved.

Other methods for measuring the density of states are available. One is to study the incoherently scattered neutron intensity from a polycrystalline sample. Then $g(\nu)$ is obtained from $\partial^2\sigma^{\mathrm{inc}}/\partial\Omega\partial\nu$ in the limit of vanishing neutron-wave-vector transfer,[2] i.e., $\vec{\kappa}\to 0$. $\partial^2\sigma^{\mathrm{inc}}/\partial\Omega\partial\nu$ is proportional to κ^2. Thus, applied to germanium, with its small incoherent cross section, this method would have worked poorly because of the necessary application of a rather large κ, which introduces systematic errors.

Roy and Brockhouse[5] recently investigated the possibility of obtaining $g(\nu)$ for strongly coherent scattering polycrystalline samples, using the incoherent approximation.[6] The intensities were measured as a function of ν for a wide range of wave-vector transfers κ and then summed over κ. Thus $g(\nu)$ could be extracted from the superposed data in the incoherent approximation. It is desirable to look more closely at this method by applying it, for example, to germanium, using much better resolution than in Ref. 5.

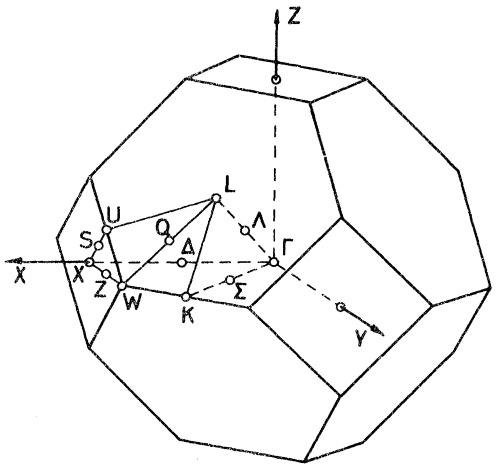

FIG. 1. Conventional notations of points and lines in the irreducible (1/48)th part of the first Brillouin zone of an fcc lattice.

II. DENSITY OF STATES

A. Experimental Frequencies

The present investigation is an extension of a previous work,[3] in which phonon dispersion relations were measured in germanium at 80 K for all principal symmetry directions and on some lines at the boundary of the Brillouin zone. Accounts of the instrument used and the experimental technique adopted will be found in Ref. 3 or in the references cited there. The accuracy of the complementary phonon frequencies is usually not as good as in Ref. 3, but the mean error of all frequencies is believed to be about 0.6%–0.8%.

The aim of the present study was to measure the frequencies of so many off-symmetry phonons that a sampling of the density of states could be performed. The phonons in a reciprocal simple-cubic-point lattice with a unit cell length of 1/10th of the distance Γ–X (Fig. 1) were studied. The original intention was to measure the frequencies of phonons corresponding to the 146 nonequivalent phonon wave vectors $\{\vec{q}_e\}$ in the irreducible 1/48th section of the first Brillouin zone for all the six branches. For lack of time it was not possible to scan all these phonons. However, in many regions of reciprocal space the topology of the phonon branches is simple, and a reduction could be made without spoiling the accuracy. More than 500 frequencies were measured and the rest of them interpolated.

In order to reduce the influence of subjectivity in the interpolation process to a minimum, the following procedure was applied: A Born–von Kármán model[7] fitted to our data of the Δ, Λ, and Σ directions[3] was used to generate frequencies of the $\{\vec{q}_e\}$ mesh. When a frequency of a point $\vec{q}_e$ had to be interpolated, the differences between the measured and calculated frequencies in the neighborhood were plotted as a function of these reciprocal points, and the value assigned to $\nu(\vec{q}_e)$ was the sum of the calculated frequency and the difference interpolated

from the plot.

The frequencies of the mesh $\{\vec{q}_e\}$ of phonon wave vectors are listed in Table I, where the principle of ordered labeling is assumed. This means that every phonon branch is assigned a number i ranging from 1 to 6. The ith branch is defined as the one of frequency $\nu_i(\vec{q})$, where $i<j$ implies $\nu_i(\vec{q}) \leq \nu_j(\vec{q})$.

B. Sampling Procedure

A number of methods exist for calculation of spectra from lattice dynamical models. A review covering the period up to 1963 will be found in Ref. 8. All procedures starting from the frequencies need a great many more frequencies than can reasonably be obtained from experiments, and it is necessary to have a mathematical device to produce a sufficient number of interpolated frequencies. Stedman *et al.*[4] obtained the spectra of aluminium and lead as follows. The boundaries of the experimental simple-cubic-point net $\{\vec{q}_e\}$ were expanded to a cube with length of side $\Gamma - X$. The cube centered at each point $\vec{q}_e$ was divided into 1000 smaller cubes defining wave vectors $\vec{q}_e^{\,n}$. Thus each phonon branch contained 1 000 000 states. By a local second-order Taylor expansion of the frequency around each point $\vec{q}_e$ with the derivatives being determined by the frequencies of $\vec{q}_e$ and its six-nearest and twelve-next-nearest neighbors every point $\vec{q}_e^{\,n}$ was assigned a frequency. $g(\nu)d\nu$ was then obtained by counting the number of states in each interval $(\nu, \nu+d\nu)$. The adopted interpolation technique works quite well in most regions of reciprocal space. When the mesh $\{\vec{q}_e\}$ is as dense as in the present case the errors in the frequencies $\nu(\vec{q}_e^{\,n})$ caused by neglecting third-order and higher terms in the Taylor expansion are small compared to the errors introduced by the measured frequencies with the present experimental accuracy. Problems will occur, for instance, when one or more of the components of $\nabla_{\vec{q}}\nu_j$ show discontinuities, as for the acoustic branches at Γ, all branches at W, accidental degeneracies, etc. In such a case, depending on whether the "corner" of $\nu_j(\vec{q})$ is directed towards higher or lower frequencies, a bump or a shift will appear in $g(\nu)$ on the low- or high-frequency side, respectively, of the frequency of the "top of the corner." This is because the "corner" will be rounded off in the interpolation. More serious, however, is the fact that the number of phonon states to be sampled, limited to 1 000 000 for every branch on account of computation time, is not large enough to avoid additional statistical scattering in the density of states. This scattering has generally been believed to be much smaller than the one caused by experimental errors in the measured frequencies. We calculated $g(\nu)d\nu$ from both the frequencies of Table I and those calculated by the Born–von Kármán model (Sec. II A). The point scattering was found to be the same in both cases and accordingly it was almost entirely caused by a too-dilute phonon point mesh. This means that the experimental errors were little reflected in the spectrum obtained, the statistical uncertainty of which mainly originated from the calculation—a situation hardly acceptable to us. An improvement of the sampling procedure was necessary.

Gilat and Dolling[9] and Gilat and Raubenheimer[10] have developed a rapid method of calculating densities of states. Its theoretical fundamentals are as follows: The irreducible section of the first Brillouin zone is divided into a uniform simple-cubic mesh of points $\vec{q}_0$. Every $\vec{q}_0$ is considered centered at a small cube. The frequency of branch j at an arbitrary point $\vec{q}_0 + \Delta\vec{q}_0$ within the cube is given by

$$\nu_j(\vec{q}_0 + \Delta\vec{q}_0) = \nu_j(\vec{q}_0) + \Delta\vec{q}_0 \cdot \nabla_{\vec{q}=\vec{q}_0}\nu_j(\vec{q}) \qquad (1)$$

if the mesh $\{\vec{q}_0\}$ is fine enough. $\nu_j(\vec{q}_0)$ belongs to a constant frequency surface passing through $\vec{q}_0$. Adding an increment $d\nu$, one will get a new surface of constant frequency through $\vec{q}_0 + \Delta\vec{q}_0$ defined by $\nu_j(\vec{q}_0) + d\nu$. The number of phonon states which lie in the range between $\nu_j(\vec{q}_0)$ and $\nu_j(\vec{q}_0) + d\nu$ is proportional to the volume dV of the layer confined by these surfaces. $g(\nu)d\nu$ is obtained by summing the phonon states (proportional to dV) over all cubes $\vec{q}_0$ (properly weighted with respect to their symmetry) for every frequency interval $(\nu, \nu+d\nu)$. The appropriate formulas are given in Ref. 10. The accuracy of the method hinges on the size of the cubes $\vec{q}_0$.

We have adopted the ideas of Gilat and co-workers to improve the sampling technique of the density of states from experimental frequencies. In a first trial we calculated $g(\nu)$ directly from the experimental mesh $\{\vec{q}_e\}$. The components of $\nabla_{\vec{q}=\vec{q}_e}\nu_j(\vec{q})$ were determined from the frequencies of the nearest neighbors around the respective points. The result was considered slightly worse than the spectrum obtained by the method of Stedman *et al.*, but with better displayed van Hove singularities. A finer-divided point mesh was necessary and an interpolation was performed with the second-order Taylor expansion, but limiting the number of new points around each $\vec{q}_e$ to 64 (1000 previously). This division led to about equal time of computation for the two methods considered. Figure 2 shows the results of branch 2 when using the Born–von Kármán frequencies of the mesh $\{\vec{q}_e\}$ in order to avoid unknown contributions from experimental errors. The new method gives a continuous curve close to the smoothed mean value of the old spectrum. Scattering of the points is replaced by considerably damped oscillations.

The final results are shown in Fig. 3 where the phonon density of states in germanium at 80 K is

TABLE I. Phonon frequencies in Ge at 80 K in units of THz.

$10\vec{q}$								
q_z	q_y	q_x	ν_1	ν_2	ν_3	ν_4	ν_5	ν_6
0	0	0	0.0	0.0	0.0	9.12	9.12	9.12
0	0	1	0.60	0.60	0.91	9.05	9.05	9.11
0	0	2	1.15	1.15	1.77	8.91	8.91	9.09
0	0	3	1.62	1.62	2.59	8.73	8.73	9.02
0	0	4	1.96	1.96	3.42	8.56	8.56	8.95
0	0	5	2.20	2.20	4.17	8.42	8.42	8.80
0	0	6	2.32	2.32	4.90	8.35	8.35	8.62
0	0	7	2.39	2.39	5.57	8.29	8.29	8.35
0	0	8	2.40	2.40	6.23	7.97	8.28	8.28
0	0	9	2.41	2.41	6.77	7.63	8.27	8.27
0	0	10	2.40	2.40	7.21	7.21	8.26	8.26
0	1	1	0.67	0.93	1.39	9.01	9.03	9.05
0	1	2	1.20	1.36	2.07	8.85	8.91	9.02
0	1	3	1.66	1.82	2.75	8.69	8.74	8.96
0	1	4	1.98	2.14	3.48	8.53	8.60	8.88
0	1	5	2.23	2.35	4.17	8.35	8.47	8.74
0	1	6	2.40	2.43	4.87	8.22	8.37	8.61
0	1	7	2.47	2.48	5.48	8.09	8.32	8.37
0	1	8	2.49	2.50	6.07	7.80	8.29	8.29
0	1	9	2.50	2.51	6.60	7.46	8.28	8.28
0	1	10	2.50	2.50	7.10	7.10	8.27	8.27
0	2	2	1.29	1.70	2.58	8.72	8.89	8.92
0	2	3	1.72	2.07	3.10	8.58	8.76	8.87
0	2	4	2.03	2.38	3.62	8.37	8.65	8.79
0	2	5	2.28	2.57	4.20	8.18	8.54	8.69
0	2	6	2.51	2.67	4.79	8.00	8.45	8.61
0	2	7	2.63	2.72	5.36	7.79	8.37	8.43
0	2	8	2.66	2.75	5.87	7.52	8.30	8.33
0	2	9	2.72	2.78	6.36	7.21	8.29	8.31
0	2	10	2.76	2.76	6.82	6.82	8.28	8.28
0	3	3	1.82	2.35	3.53	8.37	8.76	8.80
0	3	4	2.06	2.64	3.90	8.15	8.68	8.73
0	3	5	2.31	2.83	4.37	7.95	8.59	8.68
0	3	6	2.61	2.95	4.81	7.73	8.50	8.62
0	3	7	2.78	3.03	5.27	7.49	8.40	8.50
0	3	8	2.89	3.07	5.72	7.23	8.31	8.41
0	3	9	2.99	3.12	6.12	6.92	8.30	8.37
0	3	10	3.10	3.10	6.52	6.52	8.33	8.33
0	4	4	2.11	2.92	4.28	7.89	8.61	8.70
0	4	5	2.31	3.10	4.66	7.67	8.54	8.68
0	4	6	2.59	3.21	4.94	7.42	8.44	8.63
0	4	7	2.85	3.29	5.28	7.18	8.36	8.56
0	4	8	3.02	3.34	5.67	6.94	8.32	8.48
0	4	9	3.18	3.36	5.95	6.65	8.31	8.42
0	4	10	3.31	3.31	6.24	6.24	8.35	8.35
0	5	5	2.34	3.34	4.95	7.40	8.45	8.66
0	5	6	2.51	3.45	5.20	7.13	8.38	8.64
0	5	7	2.77	3.53	5.47	6.91	8.33	8.60
0	5	8	2.98	3.55	5.77	6.72	8.32	8.53
0	5	9	3.20	3.49	5.95	6.39	8.30	8.45
0	5	10	3.41	3.41	6.14	6.15	8.36	8.36
0	6	6	2.46	3.61	5.55	6.91	8.35	8.65
0	6	7	2.61	3.64	5.78	6.72	8.31	8.62
0	6	8	2.80	3.62	5.99	6.52	8.30	8.53
0	6	9	3.08	3.49	6.12	6.37	8.28	8.45
0	7	7	2.49	3.66	6.10	6.58	8.29	8.63
0	7	8	2.61	3.57	6.28	6.49	8.28	8.51
0	7	9	2.82	3.36	6.39	6.56	8.27	8.43
0	8	8	2.45	3.34	6.56	6.66	8.27	8.47

TABLE I. (*Continued*)

$10\vec{q}$								
q_z	q_y	q_x	ν_1	ν_2	ν_3	ν_4	ν_5	ν_6
0	8	9	2.57	3.09	6.69	6.78	8.26	8.38
0	9	9	2.43	2.76	6.96	6.96	8.26	8.34
1	1	1	0.86	0.86	1.73	9.02	9.02	9.03
1	1	2	1.26	1.32	2.38	8.91	8.90	8.99
1	1	3	1.62	1.82	2.94	8.79	8.77	8.93
1	1	4	1.97	2.21	3.60	8.64	8.63	8.87
1	1	5	2.20	2.46	4.19	8.48	8.53	8.75
1	1	6	2.32	2.56	4.86	8.23	8.42	8.62
1	1	7	2.41	2.62	5.48	7.98	8.35	8.48
1	1	8	2.43	2.67	6.06	7.74	8.30	8.36
1	1	9	2.44	2.70	6.54	7.43	8.27	8.31
1	2	2	1.33	1.46	2.80	8.75	8.89	8.90
1	2	3	1.66	1.92	3.31	8.60	8.76	8.87
1	2	4	1.98	2.31	3.83	8.44	8.65	8.81
1	2	5	2.24	2.62	4.33	8.24	8.56	8.72
1	2	6	2.37	2.78	4.87	8.01	8.47	8.63
1	2	7	2.48	2.91	5.39	7.76	8.40	8.51
1	2	8	2.53	3.00	5.91	7.53	8.33	8.43
1	2	9	2.59	2.99	6.32	7.16	8.28	8.40
1	3	3	1.75	2.09	3.70	8.37	8.75	8.79
1	3	4	2.02	2.44	4.14	8.18	8.66	8.74
1	3	5	2.29	2.76	4.55	7.97	8.59	8.69
1	3	6	2.46	2.98	4.95	7.73	8.52	8.63
1	3	7	2.61	3.12	5.35	7.49	8.43	8.55
1	3	8	2.74	3.27	5.77	7.24	8.36	8.46
1	3	9	2.83	3.25	6.07	6.85	8.29	8.43
1	4	4	2.07	2.61	4.46	7.91	8.63	8.70
1	4	5	2.32	2.91	4.83	7.70	8.56	8.67
1	4	6	2.55	3.15	5.13	7.46	8.48	8.63
1	4	7	2.72	3.29	5.40	7.20	8.41	8.60
1	4	8	2.91	3.44	5.70	6.93	8.36	8.49
1	4	9	3.04	3.39	5.91	6.56	8.30	8.44
1	5	5	2.28	3.05	5.12	7.43	8.48	8.68
1	5	6	2.51	3.30	5.36	7.20	8.42	8.65
1	5	7	2.70	3.42	5.57	6.95	8.36	8.58
1	5	8	2.95	3.54	5.73	6.71	8.34	8.50
1	5	9	3.14	3.46	5.87	6.41	8.31	8.44
1	6	6	2.41	3.42	5.61	6.97	8.37	8.68
1	6	7	2.59	3.57	5.79	6.77	8.32	8.61
1	6	8	2.82	3.55	5.87	6.65	8.31	8.52
1	7	7	2.47	3.64	5.98	6.74	8.29	8.64
1	7	8	2.63	3.42	6.09	6.86	8.28	8.51
1	8	8	2.47	3.21	6.29	7.05	8.27	8.48
2	2	2	1.47	1.47	3.30	8.81	8.82	8.82
2	2	3	1.65	1.69	3.75	8.60	8.78	8.80
2	2	4	1.90	2.12	4.23	8.34	8.68	8.77
2	2	5	2.10	2.54	4.62	8.10	8.57	8.72
2	2	6	2.25	2.79	5.04	7.85	8.48	8.64
2	2	7	2.37	2.96	5.47	7.60	8.40	8.56
2	2	8	2.43	3.09	5.90	7.36	8.33	8.49
2	3	3	1.75	1.84	4.20	8.43	8.74	8.75
2	3	4	1.93	2.09	4.59	8.16	8.68	8.72
2	3	5	2.11	2.46	4.91	7.91	8.58	8.70
2	3	6	2.29	2.81	5.19	7.66	8.50	8.66
2	3	7	2.43	3.06	5.53	7.38	8.42	8.58
2	3	8	2.53	3.26	5.77	7.13	8.36	8.51
2	4	4	1.98	2.28	4.90	7.97	8.65	8.70
2	4	5	2.14	2.53	5.17	7.71	8.58	8.69
2	4	6	2.33	2.84	5.37	7.44	8.51	8.65
2	4	7	2.52	3.14	5.61	7.15	8.43	8.59

TABLE I. (*Continued*)

$10\vec{q}$								
q_z	q_y	q_x	ν_1	ν_2	ν_3	ν_4	ν_5	ν_6
2	4	8	2.67	3.34	5.73	6.85	8.37	8.52
2	5	5	2.14	2.73	5.42	7.52	8.55	8.69
2	5	6	2.33	2.95	5.56	7.22	8.49	8.65
2	5	7	2.54	3.21	5.69	6.97	8.44	8.60
2	5	8	2.75	3.38	5.72	6.72	8.38	8.52
2	6	6	2.28	3.18	5.69	7.01	8.46	8.67
2	6	7	2.48	3.29	5.76	6.88	8.42	8.60
2	7	7	2.39	3.30	5.83	7.02	8.38	8.60
3	3	3	1.76	1.76	4.73	8.36	8.75	8.75
3	3	4	1.88	1.93	5.06	8.11	8.69	8.71
3	3	5	2.01	2.27	5.32	7.85	8.62	8.68
3	3	6	2.17	2.65	5.51	7.58	8.54	8.65
3	3	7	2.31	3.05	5.66	7.31	8.47	8.62
3	4	4	1.86	2.02	5.40	7.97	8.68	8.70
3	4	5	1.99	2.23	5.60	7.70	8.62	8.67
3	4	6	2.18	2.58	5.72	7.42	8.55	8.64
3	4	7	2.34	2.96	5.79	7.11	8.48	8.61
3	5	5	2.01	2.37	5.85	7.51	8.61	8.68
3	5	6	2.18	2.64	5.94	7.23	8.54	8.64
3	5	7	2.38	2.93	5.81	6.96	8.48	8.60
3	6	6	2.16	2.86	5.97	7.14	8.54	8.66
4	4	4	1.88	1.88	5.93	7.80	8.70	8.70
4	4	5	1.95	2.06	6.15	7.54	8.66	8.68
4	4	6	2.05	2.33	6.10	7.32	8.61	8.65
4	5	5	1.93	2.01	6.33	7.39	8.66	8.68
4	5	6	2.04	2.32	6.25	7.21	8.62	8.66
5	5	5	1.90	1.90	6.66	7.34	8.70	8.70

plotted together with the individual contributions from each of the six phonons branches. Oscillations due to experimental errors become increasingly important with increasing difficulty of measurement or roughly with increasing frequency. These oscillations are especially pronounced in branch six, in spite of the fact that the relative errors are smaller for optical than for acoustic phonons. However, when the dispersion is small, even small errors will be important and produce relatively large oscillations or fallacious peaks in the density of states.

C. Comparisons with Calorimetric Data

The heat capacity at constant pressure C_p has been measured for germanium by Flubacher *et al.*[11] in the temperature range 2.5 to 300 K with the experimental uncertainties of C_p estimated at 0.5% and 0.2% in the ranges 10 to 20 K and 20 to 300 K, respectively, i.e., of the same magnitudes as the errors quoted for the phonon frequencies in the present work. Below 10 K their percentage errors increase.

The largest relative errors of our density-of-states spectrum are localized to the low-frequency region. It is known that the Debye model of lattice dynamics is valid there. We calculated the heat-capacity-equivalent Debye temperature Θ_0 (reduced to absolute zero) by fitting the Debye model to the density of states up to 1 THz, below which value phonon dispersion was assumed to be absent. The result $\Theta_0 = 363$ K is in reasonable agreement with the most often quoted value 374 $\pm$ 2 K.[11]

Flubacher *et al.* deduced the specific heat at constant volume C_v from C_p by means of the formula

$$C_p - C_v = \alpha^2 TV/\chi , \qquad (2)$$

where α is the cubic coefficient of thermal expansion, V the molar volume, and χ the isothermal compressibility. They also calculated the Debye

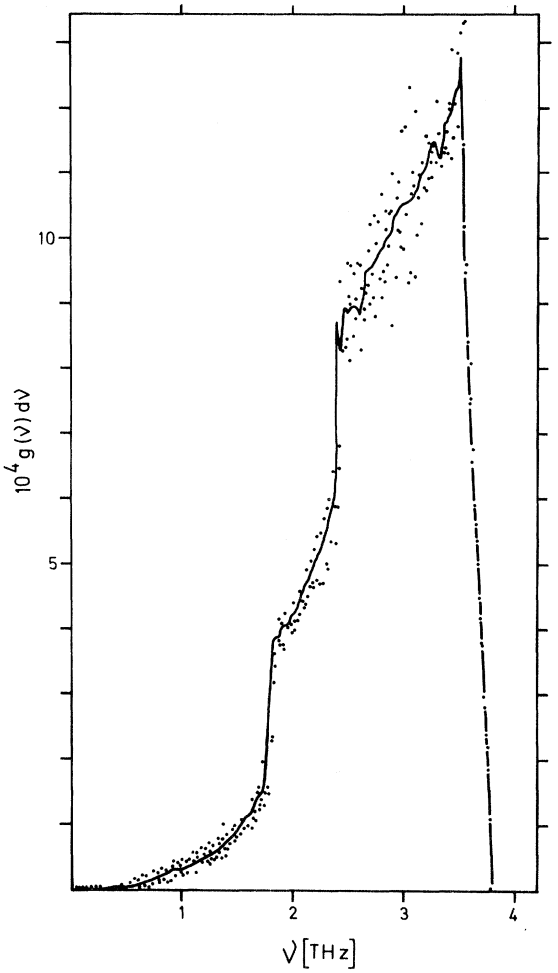

FIG. 2. Two spectra of branch 2 calculated from frequencies produced by a Born–von Kármán model by (a) the method of Stedman *et al.* (Ref. 4) (dots) and (b) the present method (solid line). In both cases $d\nu = 0.01$ THz. Some points in (a) have been deleted to obtain clearer reproduction. The solid line in (b) has not been subject to smoothing but was constructed by linear interpolation between consecutive points throughout.

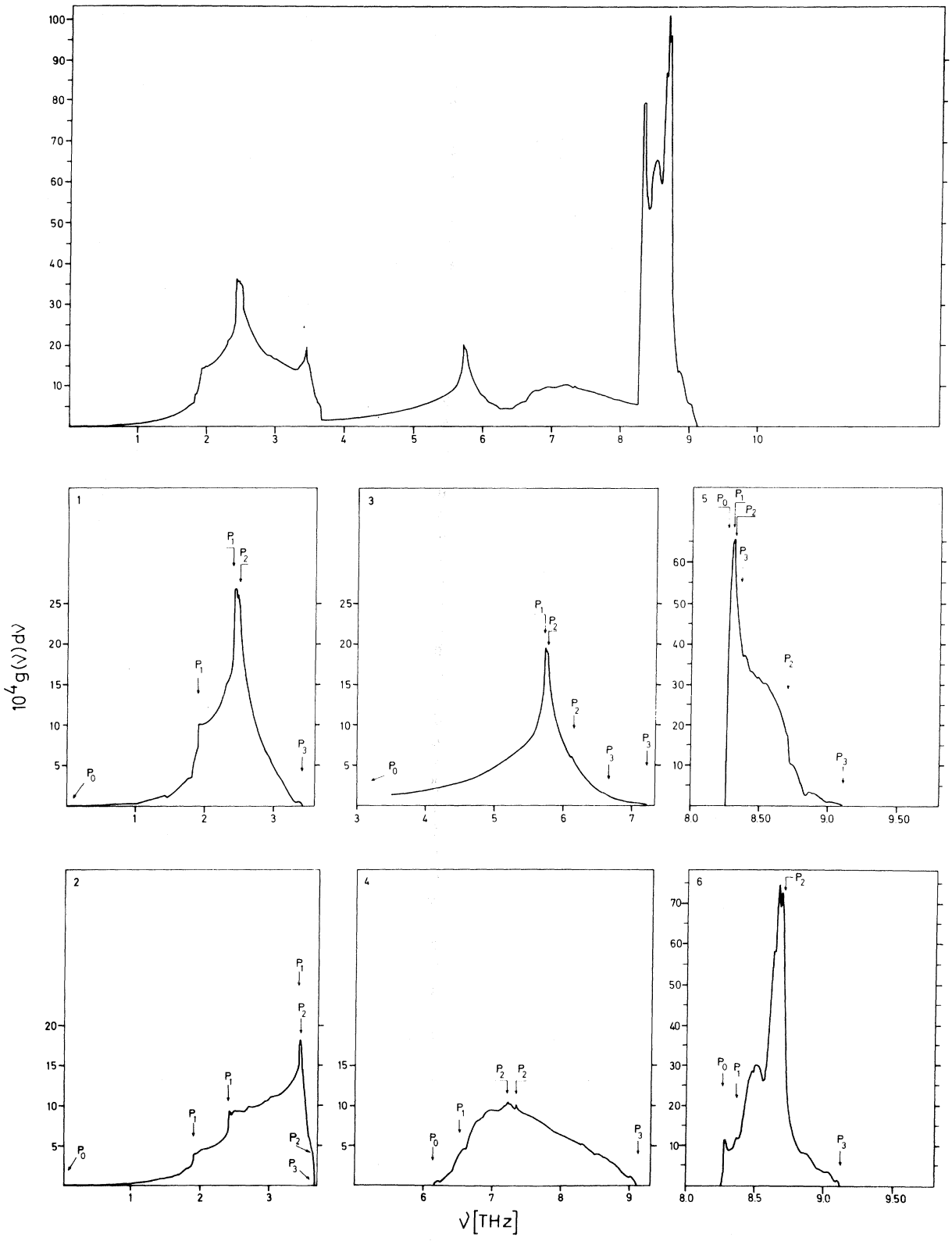

FIG. 3. The phonon density of states in Ge at 80 K as a function of frequency. Figures labeled by numbers ranging from 1 to 6 show the contributions from the respective branches. The spectra are expressed in $10^4 g(\nu)d\nu$ ($d\nu = 0.01$ THz) and the frequencies ν in units of THz. The symbols P_i mark the frequencies of the critical points listed in Table III.

temperature Θ_D equivalent to C_v and fitted the Thirring harmonic expansion

$$\Theta_D^2 = \Theta_\infty^2[1 - A(\Theta_\infty/T)^2 + B(\Theta_\infty/T)^4 - \dots] \quad (3)$$

to it. From their work it is clear that within the experimental accuracy germanium may be considered harmonic at 80 K. Thus we calculated the harmonic specific heat C_v^N for $T < 300$ K. When comparing C_v^N with the C_v of Flubacher *et al.* the temperature scale may be divided into three regions according to the behavior of the difference. In the first region, from 2.5 to 12 K, where the heat capacity drops sharply, $C_v^N < C_v$ and the difference increases percentally when approaching the lower limit. In the region between 12 and 120 K, C_v^N assumes a smoothed mean of C_v. Finally, in the third region ranging from 120 to 300 K, $C_v^N < C_v$ as is expected if anharmonicity is present. $C_v - C_v^N$ increases approximately linearly with temperature.

Flubacher *et al.* found that at about 120 K there is an abrupt onset of anharmonic contributions. It was also evident that the quasiharmonic approximation, in which the frequencies are assumed to be harmonic but are allowed to change with volume, is not sufficient to account for these contributions. Using the resulting value $\Theta_\infty = 395 \pm 3$ K they could extrapolate a C_v^F (harmonic) from their low-temperature data and calculate $C_v - C_v^F$. They found the difference to be linearly dependent on temperature and to be 1.4% of C_v at 300 K, where we get 1.6% for $(C_v - C_v^N)/C_v$.

A comparison between the moments defined by

$$\mu_n = \int_0^\infty \nu^n g(\nu)\, d\nu \quad (4)$$

which can be obtained from calorimetric data is also a sensitive check. As expected (see Table II) our lowest moments $\mu_{-2.5}$ and μ_{-2} (dominated by the very lowest frequencies) deviate from those by Flubacher *et al.* Higher moments agree well between the two measurements. Dolling and Cowley[12] fitted a second-neighbor shell model to early phonon data on germanium by Brockhouse and Iyengar and calculated the density of states and some of its moments. The present spectrum differs markedly from theirs in the region 1–4 THz. The moments μ_{-2} and μ_{-1} of Dolling and Cowley deviate considerably from ours and those of Flubacher *et al.* while higher moments agree well between the three works.

TABLE II. Moments μ_n as calculated by Flubacher *et al.* (Ref. 11) from the present data, and by Dolling and Cowley (Ref. 12).

Moments	Flubacher *et al.*	Present work	Dolling and Cowley
$\mu_{-2.5}$ (10^{-32} sec$^{5/2}$)	5.73 ± 0.03	6.4	···
μ_{-2} (10^{-26} sec^2)	7.82 ± 0.02	7.77	8.74
$\mu_{-1.5}$ (10^{-19} sec$^{3/2}$)	1.277 ± 0.003	1.274	···
μ_{-1} (10^{-13} sec)	2.314 ± 0.004	2.315	2.408
μ_{+1} (10^{12} sec^{-1})	5.82 ± 0.02	5.83	5.81
μ_{+2} (10^{25} sec^{-2})	4.06 ± 0.06	4.09	4.09
μ_{+4} (10^{51} sec^{-4})	2.50 ± 0.15	2.50	2.54
μ_{+6} (10^{77} sec^{-6})	1.75 ± 0.21	1.69	1.72

The geometric mean frequency ν_g[13] associated with the entropy is found to be 5.11 THz and the entropic Debye temperature 343 K. Flubacher *et al.* report $\nu_g = 5.110 \pm 0.015$ THz.

III. CRITICAL POINTS AND SINGULARITIES

A. Basic Theory

A striking qualitative feature of the spectra in Fig. 3 is the presence of discontinuities in $dg/d\nu$. Assuming harmonic interatomic forces van Hove[1] showed such singularities to be consequences of so-called critical points. A critical point (cp) is defined as a point $\vec{q}_c$ in reciprocal space where every component of $\nabla_{\vec{q}=\vec{q}_c} \nu_j(\vec{q})$ of a branch j is either zero or changes sign discontinuously. One distinguishes between *ordinary* cp where all derivatives are zero and *singular* cp which correspond to cross-over points between phonon branches. Ordinary cp are divided into *analytic* and *fluted*. In the vicinity of points of the first kind there exists a Taylor expansion of ν_j but not for the second. We denote a cp $\vec{q}_c$ by $P_i(n)$. The index i (= 0, 1, 2, or 3) indicates the number of principal directions in which ν_j decreases from $\nu_j(\vec{q}_c)$ and n denotes the number of discontinuous components in $\nabla_{\vec{q}=\vec{q}_c}\nu_j(\vec{q})$. The functional type of the contribution to the density of states from a cp is determined by its indices i and n. This was studied in detail by Phillips[14] who developed a procedure for determining the type of a cp: Consider a reference sphere in reciprocal space centered at the cp $\vec{q}_c$, and mark on its surface all its intersections with sectors of directions emerging from $\vec{q}_c$ with increasing and decreasing frequencies. Call these sectors positive and negative and denote their numbers by P and N, respectively. The sector numbers (P, N) completely specify the type of the cp and its topological weight q (not to be confused with wave vectors $\vec{q}$) as summarized by Phillips in the following three statements: (i) If the sector numbers are (1, 0) or (0, 1), then $q = 1$ and $j = 0$ or l, respectively, where l is the dimension of the crystal. That is, a warped (fluted) minimum or maximum is topologically equivalent to an analytic minimum or maximum, respectively. (ii) In two dimensions an (n, n) point has $j = 1$ and $q = n - 1$. (iii) In three dimensions, usually only one of P or N will be greater than 1. In the former case $j = 2$ and $q = P - 1$, and in the latter case $j = 1$ and $q = N - 1$. (In general

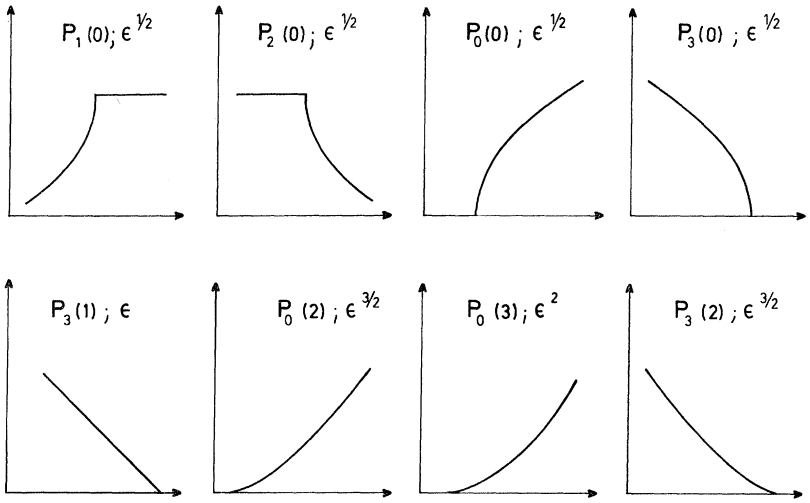

FIG. 4. The different types of contributions to the density of states from the cp encountered in this work according to Phillips (Ref. 14). $\epsilon = \nu - \nu_c$.

a point must be counted both as a $j=1$ point with $q_1 = N-1$ and as a $j=2$ point with $q_2 = P-1$.)

The existence of some critical points necessitates the existence of others. This is expressed by the Morse relations for two dimensions

$$n_0 \geq 1, \quad n_1 - n_0 \geq 1, \quad n_2 - n_1 + n_0 = 0 \tag{5}$$

and for three dimensions

$$N_0 \geq 1, \quad N_1 - N_0 \geq 2, \quad N_2 - N_1 + N_0 \geq 1,$$

$$N_3 - N_2 + N_1 - N_0 = 0\ . \tag{6}$$

The Morse number N_j (or n_j) of a cp $\vec{q}_c$ is the product of its topological weight q and its multiplicity M. Some critical points are required by symmetry and constitute the *symmetry set*. In the reciprocal lattice of a diamond structure this set is made up of the points Γ, X, L and W in three dimensions and in two by Γ, X, W, and R for $S_{\mathrm{I}}(q_z = 0)$ and Γ, X, and L for $S_{\mathrm{II}}(q_y = q_z)$ (Fig. 1). [R is the point (1, 1, 0) and its equivalences in S_{I}.] The symmetry set does not always satisfy the Morse relations. The smallest set doing this is called the *minimal set*, which need not be identical to the *true set*. Phillips pointed out that all critical points not in the symmetry set must have the weight $q = 1$.

B. Results of the Critical-Point Analysis

The results of the critical-point analysis are presented in Table III for two and three dimensions. For the latter case the table includes frequencies and, when necessary, also coordinates of the cp, all of which except one [$P_2(0)$ in branch 5 at (0.85, 0.45, 0) in S_{I}] are located on symmetry lines. Every cp encountered has the weight $q = 1$, which implies N_j (or n_j) $= M$ throughout. This means that no fluted cp are present. The symmetry set is not a minimal set for the branches 1, 2, 3, 4, and 5 in three dimensions or for 1, 2, 4, and 5 of S_{I} and 1, 2, 3, and 4 of S_{II} in two dimensions. All sets contained in Table III are minimal sets and within the limits of the experimental accuracy they are also true sets.

Johnson and Loudon[15] explicitly formulated that, if in a crystal with the diamond structure the upper branch of a degenerate pair has a $P_j(2)$ cp at W, then the lower branch must have a $P_{j+2}(2)$ cp. The present work confirms this statement.

As far as we know, this is the first attempt to obtain a cp scheme directly from experiment. Theoretical investigations have previously been published for Ge (for example Johnson and Loudon[15]), but those schemes hinge on the actual values of the parameters of the applied models, and they also differ from the present one.

C. Spectrum Singularities

The frequencies of the cp obtained have been marked in Fig. 3. Different cp contribute in different ways to the density of states. van Hove[1] and Phillips[14] worked out the expected functional behavior of these contributions as shown in Fig. 4. If $n = 0$, the point in question should give rise to a square-root frequency variation in $g(\nu)$ on one side of the critical frequency, with a linear frequency variation on the other side for P_1 and P_2 critical points. A P_0 or P_3 point should give rise to a linear contribution if $n = 1$. All P_1 and P_2 points with $n \geq 1$, or P_0 and P_3 points with $n \geq 2$, are not expected to produce discontinuities in $dg/d\nu$, but in higher-order derivatives. Thus the point W, with $n = 2$ for all branches, should not be observed in the spectrum except for the branches one and four, where it forms trivial cp. Also the cp $P_2(1)$ at X in branch four should not be revealed, but instead the cp at Γ which is trivial in branches one, two, and three.

A comparison between Table III and Figs. 3 and

TABLE III. Critical points in Ge at 80 K. Listed are $P_i(n)(P,N)$ for all cp of every branch in two and three dimensions. In the latter case the frequencies are included, and for cp not in the symmetry set the coordinates are included. Each group theoretical symbol is followed by the point multiplicity M.

Three dimensions

	$\Gamma(1)$	$X(3)$	$L(4)$	$W(6)$	$\Sigma(12)$	$Q(24)$	$L-K(U)(24)$	$S_I(24)$
1	$P_0(3)(1, 0)$	$P_1(0)(1, 2)$	$P_1(0)(1, 2)$	$P_3(2)(0, 1)$	$P_2(0)(2, 1)$			
2	$P_0(3)(1, 0)$	$P_1(0)(1, 2)$	$P_1(0)(1, 2)$	$P_1(2)(1, 2)$	$P_2(0)(2, 1)$	$P_2(0)(2, 1)$	$P_3(0)(0, 1)$	
3	$P_0(3)(1, 0)$	$P_3(1)(0, 1)$	$P_3(0)(0, 1)$	$P_2(2)(2, 1)$		$P_1(0)(1, 2)$	$P_2(0)(2, 1)$	
4	$P_3(0)(0, 1)$	$P_2(1)(2, 1)$	$P_2(0)(2, 1)$	$P_0(2)(1, 0)$	$P_1(0)(1, 2)$			
5	$P_3(0)(0, 1)$	$P_0(0)(1, 0)$	$P_2(0)(2, 1)$	$P_3(2)(0, 1)$		$P_1(0)(1, 2)$		$P_2(0)(2, 1)$
6	$P_3(0)(0, 1)$	$P_0(0)(1, 0)$	$P_2(0)(2, 1)$	$P_1(2)(1, 2)$				
1	0.00	2.40	1.90	3.41	2.49(0.7, 0.7, 0)			
2	0.00	2.40	1.90	3.41	3.66(0.65, 0.65, 0)	3.46(0.90, 0.50, 0.10)	3.68(0.69, 0.69, 0.12)	
3	0.00	7.21	6.66	6.14		5.72(0.87, 0.50, 0.13)	5.76(0.65, 0.65, 0.20)	
4	9.12	7.21	7.34	6.14	6.52(0.73, 0.73, 0)			
5	9.12	8.26	8.70	8.36		8.30(0.93, 0.50, 0.07)		8.31(0.85, 0.45, 0)
6	9.12	8.26	8.70	8.36				

Two dimensions
$s_I(q_z = 0)$

	$\Gamma(1)$	$X(2)$	$W(4)$	$R(1)$	$\Sigma(4)$	$S_I(8)$
1	$P_0(2)(1, 0)$	$P_1(0)(2, 2)$	$P_2(1)(0, 1)$	$P_0(0)(1, 0)$	$P_1(0)(2, 2)$	
2	$P_0(2)(1, 0)$	$P_1(0)(2, 2)$	$P_1(1)(2, 2)$	$P_0(0)(1, 0)$	$P_2(0)(0, 1)$	
3	$P_0(2)(1, 0)$	$P_2(1)(0, 1)$	$P_1(1)(2, 2)$	$P_2(1)(0, 1)$		
4	$P_2(0)(0, 1)$	$P_1(1)(2, 2)$	$P_0(1)(1, 0)$	$P_2(1)(0, 1)$	$P_1(0)(2, 2)$	
5	$P_2(0)(0, 1)$	$P_0(0)(1, 0)$	$P_2(1)(0, 1)$	$P_0(0)(1, 0)$		$P_1(0)(2, 2)$
6	$P_2(0)(0, 1)$	$P_0(0)(1, 0)$	$P_1(1)(2, 2)$	$P_0(0)(1, 0)$		

Two dimensions
$s_{II}(q_y = q_z)$

	$\Gamma(1)$	$X(1)$	$L(2)$	$\Sigma(2)$	$L-K(U)(4)$
1	$P_0(2)(1, 0)$	$P_1(0)(2, 2)$	$P_1(0)(2, 2)$	$P_2(0)(0, 1)$	
2	$P_0(2)(1, 0)$	$P_1(0)(2, 2)$	$P_1(0)(2, 2)$	$P_1(0)(2, 2)$	$P_2(0)(0, 1)$
3	$P_0(2)(1, 0)$	$P_2(2)(0, 1)$	$P_2(0)(0, 1)$		$P_1(0)(2, 2)$
4	$P_2(0)(0, 1)$	$P_1(2)(2, 2)$	$P_1(0)(2, 2)$	$P_0(0)(1, 0)$	
5	$P_2(0)(0, 1)$	$P_0(0)(1, 0)$	$P_1(0)(2, 2)$		
6	$P_2(0)(0, 1)$	$P_0(0)(1, 0)$	$P_1(0)(2, 2)$		

4 discloses that most of the singularities are clearly displayed, and furthermore, the frequency variations are in accordance with expectation. No singularities appear originating from points from which they were not expected. $P_3(0)$ at Γ in branch five hardly demonstrates the expected square-root frequency variation, but the oscillations due to uncertainty are pronounced in this region of $g(\nu)$. $P_2(0)$ on Q in branch two is clearly displayed, but $g(\nu)$ falls off rapidly on the other side of the critical frequency. This makes it difficult to decide whether its contribution is of type 1 or 2. In branch five the point $P_1(0)$ on Q with frequency 8.30 THz is hidden by $P_2(0)$ in S_1 of frequency 8.31 THz. This is because the contribution to $g(\nu)$ from the latter exceeds that from the former considerably. Finally, three singularities expected to be seen are more or less absent. The first is the one of $P_3(0)$ at L in branch three with frequency 6.66 THz. This may be explained as follows. Branch three has a sharp maximum at L, which means that the contribution from this region to $g(\nu)$ is small compared to those of the majority of critical regions. An inspection of the frequency surfaces shows that there are three points in reciprocal space in the vicinities of which there are far fewer points having frequencies close to the critical ones than for all other critical points. These points are precisely those which are weakly or not at all displayed in Fig. 3, namely $P_3(0)$, $P_1(0)$, and $P_2(0)$ at L, on Σ, and at L in branches three, four, and four, respectively.

ACKNOWLEDGMENTS

The authors wish to express their gratitude to Professor I. Waller for clarifying discussions in the theory of topology and to Dr. S. Rolandson for providing parts of the improved computer program.

[1]L. van Hove, Phys. Rev. 89, 1189 (1953).
[2]*Thermal Neutron Scattering*, edited by P. A. Egelstaff (Academic, New York, 1965), Chap. I and V.
[3]G. Nilsson and G. Nelin, Phys. Rev. B 3, 364 (1971).
[4]R. Stedman, L. Almquist, and G. Nilsson, Phys. Rev. 162, 549 (1967).
[5]A. P. Roy and B. N. Brockhouse, Can. J. Phys. 48, 1781 (1970).
[6]G. Placzek and L. van Hove, Phys. Rev. 93, 1207 (1954).
[7]F. Herman, J. Phys. Chem. Solids 8, 405 (1959).
[8]A. A. Maradudin *et al.*, *Solid State Physics*, Suppl. 3, edited by F. Seitz and D. Turnbull (Academic, New York, 1963).
[9]G. Gilat and G. Dolling, Phys. Letters 8, 304 (1964).
[10]G. Gilat and L. J. Raubenheimer, Phys. Rev. 144, 390 (1966).
[11]P. Flubacher, A. J. Leadbetter, and J. A. Morrison, Phil. Mag. 4, 273 (1959).
[12]G. Dolling and R. A. Cowley, Proc. Phys. Soc. (London) 88, 483 (1966).
[13]T. H. K. Barron, W. T. Berg, and J. A. Morrison, Proc. Roy. Soc. (London) A242, 478 (1957).
[14]J. C. Phillips, Phys. Rev. 104, 1263 (1956).
[15]F. A. Johnson and R. Loudon, Proc. Roy. Soc. (London) A281, 274 (1964).

PHYSICAL REVIEW B VOLUME 5, NUMBER 8 15 APRIL 1972

Electronic Effects in Elastic Constants of PbTe

A. K. Sreedhar and S. C. Gupta
Solid State Physics Laboratory, Delhi-7, India
(Received 26 October 1971)

The electronic contribution to the second- and third-order elastic constants of p-type lead telluride have been calculated as a function of temperature and carrier concentration. The results show that the electronic contribution to the elastic constants varies markedly with the carrier concentration if the nonparabolic, nonellipsoidal band model for p-PbTe is used.

I. INTRODUCTION

Keyes[1] has developed a theory for determining the electronic contribution to the elastic properties of degenerate semiconductors on the basis of the deformation-potential model.[2,3] It is shown that the electronic contribution to the elastic constants depends on the density of states function. In n-type Ge, where the bands are parabolic, the theory predicts an 8% lowering of the shear elastic constant C_{44} with attainable doping levels. In PbTe, where the bands are highly nonparabolic,[4-6] the density-of-states function increases much more rapidly with carrier energy than when the bands are parabolic. The electronic contribution to the elastic constant is therefore expected to be en-